COMMUNICATION

Photocatalytic glucose-appended bio-compatible Ir(III) anticancer complexes

Received 00th January 20xx,
Accepted 00th January 20xx

DOI: 10.1039/x0xx00000x

Zilin Zhu,[a] Li Wei,[a] Yidan Lai,[b] Oliver W. L. Carter,[c] Samya Banerjee,[d] Peter J. Sadler*[c] and Huaiyi Huang*[a]

Rationally-designed glucose-appended Ir(III) photo-catalysts ([Ir(*N,C*)$_2$(*N,N*-Glc)]$^+$, Ir1-Ir3) show visible light-induced catalytic NAD(P)H oxidation in aqueous solution. The highly *in vivo* biocompatible complex, Ir3, shows lysosome and mitochondria targeting necro-apoptotic photo-cytotoxicity against various cancer cell lines and multicellular spheroids, while remaining non-toxic in the dark.

Metal-based catalytic anti-cancer drugs are evolving as a new strategy for cancer treatment.[1,2] Advantages of this approach are (i) minimization of drug concentrations to reduce toxicity and off-target side effects, and (ii) novel mechanisms of action to overcome drug resistance, which is becoming a problem for Pt(II) chemotherapeutics.[1,2] Catalytic Rh(III), Ir(III) and Os(II) organometallic complexes can alter the intracellular redox and metabolic balance,[1,2] for example, by modifying pyruvate/lactate or NADH/NAD$^+$ (reduced and oxidized nicotinamide adenine dinucleotide) ratios within cancer cells.[1-5] The introduction of photoactivated catalysts offers the possibility of increasing selectivity for cancer cells versus normal tissues with spatially-directed light irradiation. Hence the concept of photo-catalytic cancer drugs is attractive.[1,2]

There appear to be only two literature reports to date on the design of such agents,[6,7] both Ir(III) photo-catalysts chosen for their rich photochemistry. Although the reported Ir(III) catalysts show good photo-induced intracellular NADH oxidation and anticancer activity, their poor aqueous solubility limited progress with drug development. Hence, a new generation of Ir(III) photo-catalysts with improved aqueous solubility is needed.

Here we have addressed this challenge by suitable tuning of the ligands. Glucose has been appended to an *N,N'*-donor bidentate ligand. D-Glucose (Glc) is essential for energy production in cells, and earlier reports indicate that a pendant glucose can augment the aqueous solubility of metal complexes.[8] Pendant glucose may also help increase the uptake of drug molecules into cancer cells due to the overexpression of glucose transporters (GLUTs) on cancer cell surfaces.[9] Moreover, ^{18}F-labeled 2-fluoro-2-deoxy-D-glucose (^{18}F-FDG) is commonly used in positron emission tomography/computed tomography (PET-CT) imaging to locate the exact localization of tumours.[10]

Here, we have designed and synthesized three novel D-glucose-appended cyclometalated Ir(III) complexes (**Ir1-Ir3,** Scheme 1) containing the *N,N*-Glc ligand and various *N,C*-ligands to optimize their photochemical properties, and explored the potency of their photo-catalytic anticancer activity. Complexes **Ir1-Ir3** were synthesized following the routes described in the ESI†, purified

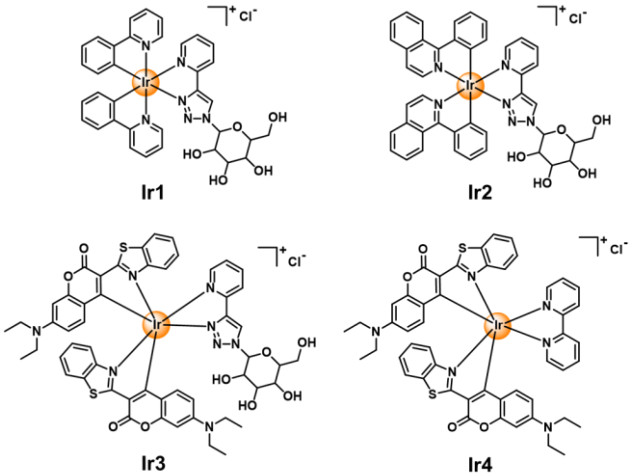

Scheme 1 Structures of the glucose-appended Ir(III) photo-catalysts (**Ir1-Ir3**) and non-glycosylated complex **Ir4**.

[a]*School of Pharmaceutical Sciences (Shenzhen), Shenzhen Campus of Sun Yat-sen University, Sun Yat-sen University, Shenzhen 518107, P. R. China.*
E-mail: huanghy87@mail.sysu.edu.cn (Dr. H. Huang)
[b]*College of Chemistry and Environmental Engineering, Shenzhen University, Shenzhen, 518060, P. R. China.*
[c]*Department of Chemistry, University of Warwick, Coventry CV4 7AL, UK*
E-mail: P.J.Sadler@warwick.ac.uk
[d]*Department of Chemistry, Indian Institute of Technology (BHU), Varanasi, UP-221005, India.*

† Electronic Supplementary Information (ESI) available: Experimental details and figures referenced throughout the text. See DOI: 10.1039/x0xx00000x

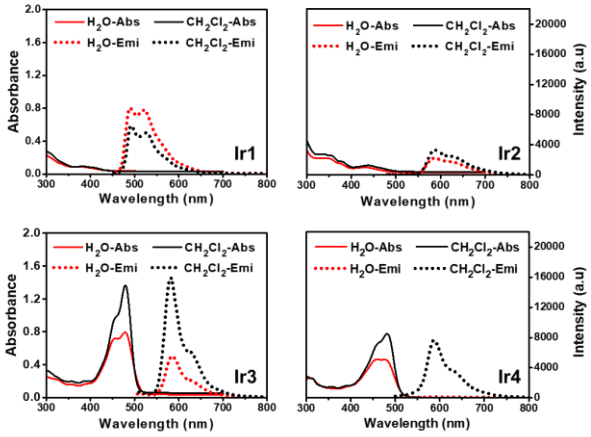

Fig. 1 UV-vis and emission spectra of **Ir1**-**Ir4** in H_2O and CH_2Cl_2 at room temperature (**Ir1**: λ_{ex} = 405 nm, **Ir2**: λ_{ex} = 458 nm and **Ir3**/**Ir4**: λ_{ex} = 488 nm, 10 μM).

by column chromatography, and characterized by ^{1}H NMR, ^{1}H-^{1}H COSY, ^{13}C NMR, HRMS and HPLC (Fig. S1-S11, ESI†), which confirmed the anticipated structures. The NMR spectra are complicated by the presence of diastereomers for complexes **Ir1-Ir3** (chiral metal and chiral glucose). The non-glycosylated control complex **Ir4**, [Ir(CO6)$_2$bpy]Cl (Scheme 1) was also synthesized and characterized (Fig. S12, ESI†) for comparison.[7]

The aqueous solubilities of **Ir1**-**Ir4** were determined (Table S1, ESI). The solubility of **Ir3** was ca. 5× higher than the related non-glycosylated complex **Ir4**. This indicates that the attachment of the pendant glucose affords reasonable aqueous solubility. The absorption bands of the complexes in various solvents were in the range of 300-550 nm (Fig. 1, Fig. S13, ESI†). These bands can be assigned as a mixture of ILCT (intra-ligand charge transfer) and MLCT (metal-to-ligand charge transfer).[11] Interestingly, introduction of the coumarin chromophore in **Ir3** resulted in bands with a significantly higher molar extinction coefficient than for **Ir1-Ir2** in the visible light range (Fig. 1, Fig. S13, ESI†). In particular, the band at ca. 480 nm is suitable for achieving visible light-induced anticancer activity. **Ir1-Ir3** exhibited green to red emission with quantum yields (excitation at 465 nm) ranging from 0.004 to 0.453 in aerated and deaerated H_2O and CH_3CN (Table S2, ESI†). Interestingly, the complexes showed much higher emission quantum yields in de-aerated H_2O or CH_2Cl_2 than in aerated solutions (Fig. S14, ESI), indicating possible interactions between the excited state complexes and O_2. Such interactions might generate reactive oxygen species (ROS), which are known to damage cancer cells via oxidative stress.[12] Importantly, the complexes exhibited better photo-stability compared to the clinically-used photosensitizer Chlorin e6 (Ce6) (Fig. 2a, Fig. S15, ESI†). The photo-stability of **Ir3** was slightly lower than **Ir1-Ir2**, however, the extremely high light absorption efficiency of **Ir3** is essential to achieve effective in-cell photo-catalysis.

Molecular lipophilicity, which plays an important role in cellular drug uptake, was determined by measuring the distribution coefficient (log P) in octanol-water mixtures. The log P values for **Ir1-Ir4** were determined to be 0.18, 0.31, 0.32 and 1.34, respectively (Fig. 2b and Table S3, ESI†), indicating the higher hydrophilicity of the glucose-appended complex **Ir3** when compared with the non-glycosylated complex **Ir4**. These data also indicate that **Ir2** and **Ir3** are more lipophilic than **Ir1** and thus might penetrate cancer cell lipid bilayer membranes more easily.

The singlet oxygen generation ($^1O_2$) quantum yields (Φ_Δ) of **Ir1**-**Ir3** (A_{465nm} = 0.1) were determined in aqueous solution using 9,10-anthracenediylbis-(methylene)dimalonic acid (ABDA) as the $^1O_2$ probe (Fig. S16-S17, ESI†). The absorbance of ABDA dramatically decreased upon 465 nm light irradiation in the presence of **Ir1-Ir3** (Fig. S16, ESI†), implying the efficient $^1O_2$ generation ability of Ir(III) complexes. The quantum yields were 0.06 for **Ir1**, 0.39 for **Ir2** and 0.23 for **Ir3** with [Ru(bpy)$_3$]Cl$_2$ as the standard (Φ_Δ = 0.18 in H_2O) (Fig. 2c, Table S4, ESI†). These Φ_Δ values suggest that these complexes could act as photosensitizers for PDT applications. Interestingly, **Ir3** also induced effective $^1O_2$ generation even on 525 nm green light irradiation (Φ_Δ = XXX), while the control complex, [Ru(bpy)$_3$]Cl$_2$ was weak in generating $^1O_2$ under green light (Fig. S18, ESI†).

NADH and NADPH are important coenzymes in living cells which also participate in the maintenance of the intracellular redox balance.[6,7] Recently, we reported intracellular NAD(P)H photo-oxidation by Ir(III)-based anticancer agents, which in turn generated H_2O_2 as the intracellular ROS. The in-cell NAD(P)H photo-oxidation disrupted the redox homeostasis and ultimately induced oxidative stress-related cell death.[6,7] Three Ir(III) complexes (**Ir1-Ir2**, 5 μM; **Ir3**, 0.5 μM) reported here were tested as photo-catalysts for NAD(P)H oxidation under 465 nm light irradiation by monitoring the change of characteristic absorbance peak of NADH and NADPH at 339 nm (Fig. S19, ESI†). The highest measured NADH/NADPH catalytic turnover numbers (TON) were 207.1/203.3, with turnover frequencies (TOF) of 414.2/406.6 for **Ir3** (Fig. 2d and Table S5, ESI†), indicating that **Ir3** is 4× and 1.5× more potent as a photo-catalyst for NAD(P)H oxidation compared to the reported complexes

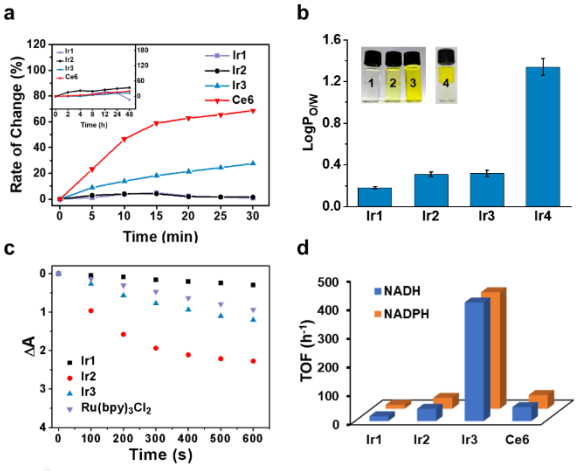

Fig. 2 (a) Study of the photo-stability of **Ir1-Ir3** and Chlorin e6 under light exposure of various times. Inset: Study of the dark-stability in 48 h. [change in the λ_{max} was monitored at 300 nm (for **Ir1**/**Ir2**), 484 nm (for **Ir3**) and 402 nm (for Ce6 respectively] (b) Octanol/water partition coefficients of **Ir1-Ir4**. Inset: Image of distribution of **Ir1-Ir4**. (c) Comparison of $^1O_2$ generation for **Ir1-Ir3** and standard [Ru(bpy)$_3$]Cl$_2$ in aqueous solution by determining the time dependent change in the absorbance of ABDA. (d) Turnover frequency of **Ir1-Ir3** for NAD(P)H (160 μM) photo-oxidation after 30 min irradiation.

Table 1. IC_{50} values (μM) and phototoxic indices (PI) for **Ir1-Ir4**, 5-ALA and cisplatin against HeLa cells.

Complex	Dark[a]	Light[b]	PI[c]
Ir1	>100	11.7 ± 0.3	>8.5
Ir2	>100	1.2 ± 0.04	>83.3
Ir3	26.7 ± 0.7	0.08 ± 0.003	333.8
Ir4	0.7 ± 0.03	0.2 ± 0.01	3.5
5-ALA	>1000	215.8 ± 3.5	>4.6
Cisplatin	18.7 ± 1.1	17.9 ± 0.9	1.0

[a]48 h drug exposure in the dark at 37 °C, 5% CO_2 in the dark. [b]16 h drug exposure, followed by light irradiation (465 nm, 11.7 J/cm^2) and then 32 h incubation at 37 °C, 5% CO_2 in the dark. [c]PI = $IC_{50(Dark)}/IC_{50(light)}$. 5-ALA = 5-aminolevulinic acid.

$[Ir(ttpy)(pq)Cl]PF_6$ (ttpy = 4′-(p-tolyl)-2,2′:6′,2′-terpyridine; pq= 3-phenylisoquinoline)[6] and $[Ir(CO6)_2(bpy(CH_2N(CH_3)_3)_2](PF_6)_3$ (CO6 = coumarin 6 and $bpyCH_2N(CH_3)_3$ = 4,4′-bis(N,N,N-trimethyl-methanaminium)-2,2′-biyridine)[7], respectively. On the contrary, the complexes did not induce any evident NAD(P)H oxidation in the dark, indicating the necessity of light. Interestingly, **Ir3** exhibited higher catalytic efficiency than Chlorin e6 and achieved the maximum TON within a very short period of light irradiation, sharply differing from **Ir1** and **Ir2** (Fig. S20, ESI†). The photo-oxidation of NAD(P)H was associated with the generation of H_2O_2, as detected by an H_2O_2 test paper (Fig. S21, ESI†), indicating the involvement of O_2 in the process of photo-catalysis. The above observation indicates that O_2 is most likely converted to H_2O_2 via the superoxide radical anion $O_2^{\cdot-}$.[6]

Since complexes **Ir1-Ir3** exhibited both photo-induced $^1O_2$ production and NAD(P)H oxidative activity, we further explored their photo-cytotoxicity against three cancer cell lines (HeLa cervical, A549 lung and B16 melanoma). Clinically used chemotherapeutic drug cisplatin and photosensitizer pro-drug 5-ALA were used as positive controls, and cells incubated with the complexes in the dark alone were used as negative controls. After 16 h drug incubation time, followed by 5 min irradiation (465 nm light, irradiance 11.7 J/cm^2) without replacing the medium and a further 32 h recovery, the photo-toxicity of the complexes was measured. The dark-treated cells were incubated with compounds for 48 h. The complexes exhibited remarkable photo-toxicity (Table 1, Table S6, ESI†) with high photo-toxicity indices (PI = $IC_{50(Dark)}$/ $IC_{50(light)}$).

Importantly, **Ir3** gave a PI = 333.8, ca. 73× higher than the clinical photosensitizer 5-aminolevulinic acid (5-ALA) against HeLa cells. Cisplatin is not a photosensitizer and did not give rise to any significant increase in toxicity after light irradiation (Table 1 and Table S6, ESI†). Interestingly, complex **Ir3** also exhibited nanomolar dark and phototoxicity in B16 melanoma cells, with a $IC_{50(light)}$ value of *ca.* 2.0 nM. We also compared the cytotoxicity of **Ir1**-**Ir3** with the non-glycosylated analogue (**Ir4**) (Table 1). From Table 1, it is clear that the addition of the N,N-Glc ligand decreases the dark toxicity and also augments the photo-cytotoxicity of the complexes. The mechanism of photo-cytotoxicity requires further investigation and HeLa cells were selected for studies of the photo-therapeutic mechanism. [13]

Cellular uptake can influence drug activity.[6,7] To investigate the uptake profile of complexes **Ir1-Ir3** in HeLa cells, intracellular complex-based emission intensity was monitored at various time

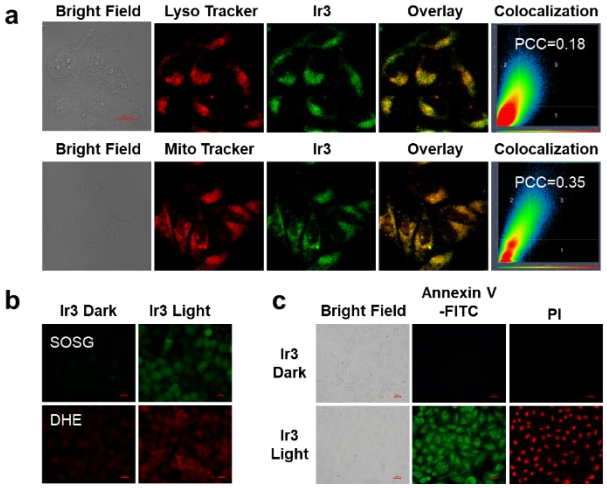

Fig. 3 (a) Confocal imaging showing the co-localization of **Ir3** with either LTDR or MTR in living HeLa cells incubated with **Ir3** (10 μM). λ_{ex} = 488 nm, λ_{em} = 580 ± 40 nm. Scale bar: 20 μm. (b) Light induced ROS generation in HeLa cells by **Ir3** using DHE and SOSG as the $O_2^{\cdot-}$ and $^1O_2$ probes, respectively. Scale bars: 20 μm. (c) Detection of cell death mechanism of **Ir3** by annexin V-FITC/PI assay. Scale bars: 20 μm.

points using flow cytometry. As shown in Fig. S22 (ESI†), the complexes showed a time dependent intracellular uptake profile. Subsequent co-localization imaging with commercial dyes Mito Tracker Red (MTR) and Lyso Tracker Deep Red (LTDR) indicated that **Ir1** and **Ir2** mainly localizes in lysosomes, whereas **Ir3** is located in both lysosomes and mitochondria (Fig. 3a and Fig. S23, ESI†). Such non-nuclear localization of the complexes might be helpful for overcoming drug resistance. In contrast, NER (nucleotide excision repair) is one of the factors responsible for cisplatin resistance.[14]

To confirm that photo-triggered cell death is induced by intracellular ROS production via both the type I (ROS) and type II ($^1O_2$) mechanisms,[7] intracellular ROS generation was monitored by Singlet Oxygen Sensor Green (SOSG) and dihydroethidium (DHE) staining assays.[15] The photo-induced intracellular $^1O_2$ generation by **Ir2** and **Ir3** was evident from the intracellular green fluorescence of SOSG (Fig. 3b, and Fig. S24, ESI†). In addition, notable DHE fluorescence was also detected in HeLa cells upon light exposure, indicating generation of superoxide radicals (Fig. S25, ESI†). These observations correlate well with the observed aqueous solution behavior described above.

The photo-triggered intracellular ROS generation resulted in mitochondrial depolarization, as was evident from the enhancement and decrease of intracellular green and red fluorescence, respectively, in the JC-1 assay with **Ir2** and **Ir3** where carbonyl cyanide m-chlorophenyl hydrazone (CCCP) was used as the positive control (Fig. S26, ESI†). Notably, no such change in the mitochondrial membrane potential was observed in the dark in presence of **Ir1-Ir3**. Blue 465 nm light induced intracellular ROS generation, and mitochondrial depolarization by **Ir2** and **Ir3** ultimately caused necro-apoptotic cancer cell death as was evident from the Annexin V-FITC/Propidium Iodide assay (Fig. 3c, Fig. S27, ESI†). The cell death mechanism was also quantitatively analyzed by Annexin V-FITC/PI assay using flow cytometry (Fig. S28, ESI†). **Ir3** (5 μM) in the dark did not induce any significant cell death, but was found to induce ca. 15% early apoptotic and ca. 9% necro-apoptotic cell death on light exposure.

The photo-cytotoxicity of **Ir3** was evaluated against 3D multicellular spheroids (MCTSs), which have a hypoxic core, in view of the favorable 2D *in*

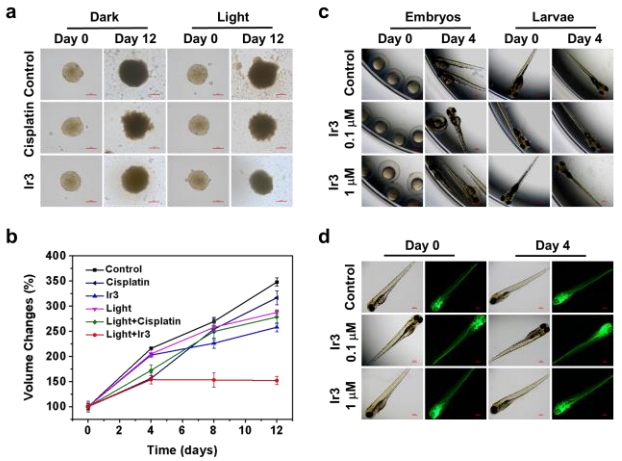

Fig. 4 (a) Representative microscopy images of multicellular HeLa spheroids showing growth inhibition no treatment (only culture medium, control), cisplatin (50 μM) or complex **Ir3** (5 μM) treatment, with or without light irradiation. (b) Volume change curves of MCTSs after various treatments over 12 days. The error bars denote the standard deviation of three parallel MCTSs. (c) Development and survival assay in wild-type zebrafish embryos and larvae after treatment with **Ir3** for 4 days, indicating the *in vivo* biocompatibility of **Ir3**. (d) Blood vessel morphology in *Tg(flk1:EGFP)*^{s843} zebrafish larvae after treatment with **Ir3** for 4 days. Scale bars: 200 μm.

vitro photo-activated anticancer profile of this complex. Recently, MCTSs have emerged as useful mimics of solid tumors with complicated microenvironments.[16] Here, we utilized MCTSs of diameter ca. 400 μm. It is challenging to deliver the drug into the core of the MCTSs as the drug has to pass through many layers of cells. As shown in Fig. S29 (ESI†), by Z-stack scanning, the core of **Ir3** (5 μM)-treated MCTSs is illuminated after 24 h of incubation, implying that **Ir3** can efficiently penetrate MCTSs. Moreover, as shown in Fig. 4a, 4b and Fig. S30 (ESI†), **Ir3** on light irradiation significantly inhibited the growth of MCTSs compared to the untreated control. In the dark, **Ir3** slightly suppressed the growth of MCTSs. Moreover, **Ir3** (5 μM) on light irradiation gave rise to higher antitumor activity than cisplatin (50 μM) in the dark.

Zebrafish have attracted significant attention as a vertebrate model to test drug toxicity *in vivo*.[17] We evaluated the toxicity of **Ir3** by exposing zebrafish embryos and larvae to various concentrations of aqueous **Ir3** in the dark. Remarkably, the survival rate of embryos and larvae was ca. 100% even after four days of exposure to 1 μM (500× light IC_{50} in B16 cells) of **Ir3** (Fig. 4c and Fig. S31, ESI†), revealing the high *in vivo* biocompatibility of **Ir3**. To investigate the effect of **Ir3** on blood vessels, we used the *Tg(flk1:EGFP)*^{s843} zebrafish model[18], which has green fluorescence labelled blood vessels. As shown in Fig. 4d, **Ir3** (1 μM) did not cause any substantial damage to blood vessels, again indicating its *in vivo* biocompatibility. Overall, these results indicate that **Ir3** without any light exposure can remain dormant *in vivo*, allowing activation at the target site upon light exposure. These observations suggest that **Ir3** has appropriate *in vivo* biosafety and the potential to overcome the side effects of cisplatin.

In summary, we have described three novel Ir(III) photo-catalysts (**Ir1**-**Ir3**) which are active as anticancer agents when irradiated by visible light. Attachment of the pendant glucose increased the aqueous solubility of the complexes. The complexes showed efficient NAD(P)H photo-oxidation under blue light. For blue light induced NAD(P)H photo-oxidation, the TON and TOF of **Ir3** were ca. 4× times higher than for previously reported Ir(III) complexes.[6,7] Hence ligand tuning has a significant role in controlling the catalytic activity of this class of Ir(III) complexes. The complexes show mitochondria/lysosome targeting, with necro-apoptotic photo- cytotoxicity at sub-micromolar concentrations via ROS generation and NAD(P)H oxidation. Interestingly, **Ir3** is highly biocompatible in the dark, as was evident from the *in vivo* zebrafish studies. The complex has the potential to minimize side effects, and with its novel mechanism of action, to overcome the problem of resistance which can develop for cisplatin. Since hypoxia contributes to cancer drug resistance, **Ir3** is expected to provide a platform of drug development to treat hypoxic tumours as this complex also effectively inhibited 3D multicellular spheroid growth. The detailed anticancer mechanism under hypoxia will be the subject of our future research.

Conflicts of interest

There are no conflicts to declare.

Acknowledgements

This work was supported by National Natural Science Foundation of China (NSFC 22007104), the Fundamental Research Funds for the Central Universities (22lgqb37), Project of the Natural Science Foundation of Guangdong Province (2019A1515110601, 2021B1515020050) Science, Technology and Innovation Commission of Shenzhen Municipality Project (JCYJ20190807152616996), “Summit Plan” High level hospital construction project of Foshan (FSSYKF-2020002) and DST, Government of India (DST/INSPIRE/04/2019/000492). We thank the EPSRC (grant no. EP/P030572/1, EP/N033191/1 and PhD CASE Award for OWLC) and GoldenKeys High-Tech Materials Co., Ltd. for their support for a PhD CASE award through the EPSRC Centre for Doctoral Training in Molecular Analytical Science for OWLC.

References

1. S. Banerjee and P. J. Sadler, *RSC Chem. Biol.*, 2021, **2**, 12.
2. Z. Fan, J. Huang, H. Huang and S. Banerjee, *ChemMedChem*, 2021, **16**, 2480.
3. W. -Y. Zhang, H. E. Bridgewater, S. Banerjee, J. J. Soldevila-Barreda, G. J. Clarkson, H. Shi, C. Imberti and P. J. Sadler, *Eur. J. Inorg. Chem.*, 2020, 1052.
4. J. J. Soldevila-Barreda, I. Romero-Canelo´n, A. Habtemariam and P. J. Sadler, *Nat. Commun.*, 2015, ***6***, 6582.
5. J. P. C. Coverdale, I. Romero-Canelo´n, C. Sanchez-Cano, G. J. Clarkson, A. Habtemariam, M. Wills and P. J. Sadler, *Nat. Chem.*, 2018, **10**, 347.

6. H. Huang, S. Banerjee, K. Qiu, P. Zhang, O. Blacque, T. Malcomson, M. J. Paterson, G. J. Clarkson, M. Staniforth, V. G. Stavros, G. Gasser, H. Chao and P. J. Sadler, *Nat. Chem.*, 2019, **11**, 1041.
7. C. Huang, C. Liang, T. Sadhukhan, S. Banerjee, Z. Fan, T. Li, Z. Zhu, P. Zhang, K. Raghavachari, H. Huang, *Angew. Chem. Int. Ed.*, 2021, **60**, 9474.
8. J. Liu, X. Liao, K. Xiong, S. Kuang, C. Jin, L. Ji, H. Chao, *Chem. Commun.*, 2020, **56**, 5839.
9. M. Patra, S. G. Awuah and S. J. Lippard, *J. Am. Chem. Soc.*, 2016, **138**, 12541.
10. C. Plathow and W. A. Weber, *J. Nucl. Med.*, 2008, **49**, 43S.
11. Q. Zhao, C. Huang and F. Li, *Chem. Soc. Rev.*, 2011, **40**, 2508.
12. J. S. Nam, M. G. Kang, J. Kang, S. Y. Park, S. J. C. Lee, H. T. Kim, J. K. Seo, O. H. Kwon, M. H. Lim, H. W. Rhee and T. H. Kwon, *J. Am. Chem. Soc.*, 2016, **138**, 10968.
13. X. Zhao, J. Liu, J. Fan, H. Chao and X. Peng. *Chem. Soc. Rev.*, 2021, **50**, 4185.
14. I. Schreck, D. Chudziak, S. Schneider, A. Seidel, K. L. Platt, F. Oesch and C. Weiss, *Toxicology*, 2009, **259**, 91.
15. S. Monro, K. L. Colón, H. Yin, J. Roque, P. Konda, S. Gujar, R. P. Thummel, L. Lilge, C. G. Cameron, S. A. McFarland, *Chem. Rev.*, 2019, **119**, 797.
16. J. Karges, S. Kuang, F. Maschietto, O. Blacque, I. Ciofini, H. Chao and G. Gasser, *Nat. Commun.*, 2020, **11**, 3262.
17. K. Bambino and J. Chu, Curr. *Top. Dev. Biol.*, 2017, **124**, 331.
18. S. Jin, D. Beis, T. Mitchel, J. Chen and D. Y. R. Stainier, *Development*, 2005, **132**, 5199.

